



Resveratrol and Gold Nanoparticles Combination Downregulate Livin in Hepatocellular Carcinoma Rat Model

Heba Bassiony¹, Sahar Elsheikh², Yasser Ezzat Shahein², Salwa Sabet¹, Haidan M. El-Shorbagy^{*1,3}

¹Zoology Department, Faculty of Science, Cairo University, Giza 12613, Egypt

²Molecular Biology Department, Biotechnology Research Institute, National Research Centre, Dokki, Cairo, 12622, Egypt

³Faculty of Biotechnology, October University for Modern Science and Arts, 6th October, Giza, Egypt



Abstract

Hepatocellular carcinoma (HCC) has reported high prevalence rates recently in Egypt and worldwide. Livin is one of the apoptotic inhibitor genes and its silencing increases the apoptotic incidence and hence the resistance to cancer proliferation. Resveratrol (Res) and gold nanoparticles (Au-NPs) have been documented for their antitumor activities. In the present study, we used hepatocarcinoma as a model to investigate the combination of Res and Au-NPs (Res-Au-NPs) antitumor activity, via their effect on the expression of livin' and A-fetoprotein genes (AFP). Au-NPs (size: 50.0±2.0 nm) were produced by the seeded growth technique. The HCC rat model was administered with Res, Au-NPs, and their combination for two months. Livin and AFP gene expressions, DNA damage, and pathological changes in the liver tissues were assessed. Our results revealed a significant reduction in livin' and AFP mRNA expression levels in HCC rats treated with a combination of Res and Au-NPs compared to those treated with Res or Au-NPs alone. This reduction was accompanied by increased DNA damage in the same group. The histological examination revealed an improvement in parenchymal structure with decreased degenerated hepatocytes in the Res-Au-NPs treated group compared to HCC, Res, and Au-NPs groups. In conclusion, the combination of Res and Au-NPs might be more effective in HCC treatment than using Res or Au-NPs alone due to the synergetic effects of both, which might be a prospective directed approach for the treatment of HCC.

Keywords: Livin; Resveratrol; Gold nanoparticles; Hepatocellular carcinoma

1. Introduction

Hepatocellular carcinoma (HCC) is the sixth most widespread cancer disease universally and it ranks fourth among the cancer diseases causing death [1]. Egypt is the third most popular country in the prevalence of Hepatocellular carcinoma (HCC) among African countries [2]. The increased survival rate of cirrhosis and incidence of HCV are considered the main risk factors for developing HCC [3-5].

Livin or Baculoviral IAP repeat-containing 7 (*BIRC7*) is one of the apoptosis protein family inhibitors (IAP), which may develop many types of cancer via disturbing cell cycle and cell proliferation by inhibiting the programmed cell death, it is thought to be an antiapoptotic oncogene. Besides, it is a key regulator of apoptosis, cytokinesis, and signal transduction [6-8]. *BIRC7* protein is composed of one

zinc-binding ring domain and one Baculovirus IAP-Repeat (BIR) domain consisting of 70 amino acids which are responsible for the inhibitory effect via reacting with APAF1 and caspases together with cytochrome C to arbitrate caspase 9 activation [9]. Livin protein was detected to be overexpressed in many cancer types especially those associated with chemoresistance and malignancy in colorectal cancer, renal carcinoma, papillary thyroid carcinoma, adrenocortical tumors, hepatocellular carcinoma, and prostate cancer [10-16]. Livin is considered as a new biomarker for colorectal and colon cancer screening as it can detect colon cancer at the early stage accurately [17, 18]. Recently, elevated expression of livin was reported to be associated with cell migration, invasion, proliferation, aggressiveness of tumor, metastasis and poor prognosis in colon cancer

Corresponding author: haidan@sci.cu.edu.eg

Receive Date: 26 July 2023 Revise Date: 01 October 2023, Accept Date: 05 November 2023

DOI: [10.21608/EJCHEM.2023.224111.8313](https://doi.org/10.21608/EJCHEM.2023.224111.8313)

©2024 National Information and Documentation Center (NIDOC)

[16, 17]. Moreover, an association between overexpression of livin and bad prognosis with low survival rate in HCC associated with HCV was recently reported [19].

Biomarkers are well known for their significant role as a predictive and prognostic tool [20]. A-fetoprotein (AFP) is a serum biomarker used for the diagnosis and monitoring of HCC postoperatively [21]. Thus AFP is considered one of the most popular diagnostic tools for HCC, with some limitations as its level was reported to be elevated in testicular cancer, pregnancy, and some chronic diseases like cirrhosis and hepatitis [22].

Resveratrol (Res), a natural polyphenol phytoalexin compound found in grapes, berries, and peanuts has been recently detected to have a management role in many cancer types like B-cell malignancies, oral squamous cell carcinoma, lymphangioliomyomatosis, and triple-negative breast cancer through different genomic pathways [23-26]. Res was previously reported to be a vital inducer of autophagy and a good regulator of the epigenome and transcriptome [27-32]. Further, Res has demonstrated to be involved in DNA damage-induced cancer cell aging via regulating the p53-CXCR2 pathway through increasing the reactive oxygen species (ROS) production and thus DNA damage response (DDR) protein in U2OS cells [33]. Moreover, in xenograft mice, the tumor was inhibited via enhancing apoptosis by inhibiting VEGF, COX-2, and cyclin D1 [34].

The advent of nanomedicine has steered away from chemotherapy to highlight treatment on the molecular level as a powerful agent to fight tumor resistance and intractable diseases [35, 36]. Gold nanoparticles (Au-NPs) tiny size permit their passage to the cancer cell through its leaky blood vessels and lymphatic system which facilitates their uptake and accordingly, Au-NPs accumulation that improves their retention effect [37]. The great ratio of surface area relative to the volume of Au-NPs offers a special platform to label or coat numerous functional objects on their surface. Various functionalization of (Au-NPs) offered them wide application in nanomedicine, bioimaging, drug delivery and cancer treatment. For example, Au-NPs proved their efficiency as an antitumor agent and as a delivery system of siRNA to prostate cancer [38]. Several recent *invitro* studies have reported the inhibitory, antineoplastic and antioxidant effects of Au-NPs Cervical, Melanoma

Cancer Cell, and MCF-7 cell line Lines [39-41]. Interestingly, several shapes and sizes of Au-NPs have been reported for their efficiency in gene silencing [42-44].

The present study aimed to assess the efficiency of silencing livin gene by resveratrol formulated gold nanoparticles (AuNPs) *in vivo*, as a therapeutic tool to treat HCC using Diethylnitrosamine-induced hepatocellular carcinoma rat as a model.

2- Experimental

Chemicals

Analytical-grade chemicals were obtained from Sigma Aldrich Company. Cairo, Egypt. We bought Molecular Kits from Thermo Scientific, Inc. in the USA.

Preparation and characterization of AuNPs

AuNPs with 50 ± 2.0 nm size were synthesized by seeded growth method; where 5ml of 0.2M CTAB solution and 1.5ml HAuCl₄ (1M) were mixed and vigorously stirred under dark condition. For production of seeded solution, 0.6 mL of 0.01M ice-cold (0.01 M) NaBH₄ was added to the solution resulting in converting the color of the solution into brownish yellow with continuing vigorous stirring for another two minutes at 25°C [45]. At 25 °C, 0.35 mL of 0.004 M AgNO₃ was gently mixed with 10 mL of growth solution containing 5 ml of 0.001M HAuCl and 5 ml of 0.20 M CTAB in a clean test tube, followed by the addition of 70 ml of 0.0788 M ascorbic acid and 5 ml of 1 M HCl. Finally, 12 μ L of the previously prepared seed solution were added at the center of the growth solution resulting in changing the colour of the solution progressively within 10 to 20 minutes. Throughout the steps of the preparation experiment, the growth solution's temperature was maintained at 27- 30°C.

High-resolution transmission electron microscopy was used to characterize the physico-chemical properties of AuNPs (HR-TEM, Tecnica G2, Super twin, double tilt, FEI, Netherlands). Inductively Coupled Plasma-Optical Emission Spectroscopy (ICP-OE) particle size analyzer and Zeta potential measurements (Zeta sizer nanoseries'zs', Malvern, UK) were used to.

Animals

From the National Cancer Institute (NCI) 6-week-old Wistar albino male rats weighting 120-150 g were purchased. All experimental methods were

carried out in compliance with the international standards for the care and use of laboratory animals.

Before the experiment began, rats were given one week to acclimatize after being randomly assigned to plastic cages with sawdust bedding upon arrival. They were given access to food and water *ad libitum* and housed in a typical environment of room temperature (22-24 °C), humidity (45-65%), and light (12 hr. light/12 hr. dark cycles). Six equal groups of six rats each were assigned by the following labels:

-ve HCC, -ve Res untreated, HCC, Res, Au-NPs, and Res +Au-NPs.

Experimental design

Rats were divided into six groups; -ve HCC group: rats received single intraperitoneal injection of saline followed by subcutaneous injections of corn oil twice weekly for 12 weeks, -ve Res group: rats orally received 0.5% aqueous solution of carboxymethyl cellulose (CMC) daily for 15 day before tumour progression and after HCC for two weeks, HCC group: rats receive single intraperitoneal injection of diethyl nitrosamine (200 mg/kg body weight), next CCl₄ injections subcutaneously (3mL/kg body weight)twice weekly for 12 weeks, Res group: rats orally received 20 mg/kg of Resveratrol (Res) dissolved in 0.5% aqueous solution of CMC daily for 15 days after tumour progression for two weeks, Au

NPs group:after tumor progression rats were treated with 0.5ml of Au-NPs for two weeks, Res-AuNPs group: tumour bearing rats orally received 20 mg/kg of Res dissolved in 0.5% aqueous solution of CMC daily for two weeks simultaneously with intravenous injection of Au-NPs in tail vein of rat after tumor progression.

Expression levels of the AFP and Livin genes

By using Thermo Scientific RNA Purification Kit, total RNA was isolated from frozen samples of liver tissue then was kept at -80 according to the manufacturer's recommendations. Remaining genomic DNA was removed using DNase I treatment before EDTA treatment. cDNA synthesis was performed using 1 mg extracted RNA according to the manufacturer's recommendation of RevertAid First Strand cDNA Synthesis Kit. The produced cDNA was utilized to measure the expression levels of AFP and Livin genes using DreamTaq Green PCR Master Mix (2x) via Real-time PCR in 25 ml total volume reaction [46]. The thermal cycler PCR (Techne TC-3000) was used to run the reaction for 35 cycles at annealing temperature 60 °C for AFP, Livin, and GAPDH. Table 1 lists the amplification primers that were employed. Gene values were scaled to GAPDH as an internal control where samples for each gene were prepared in triplicate.

Table 1: Primer sequences used for QRT-PCR

Gene	Sense 5'-3'	Antisense 3'-5'
H GAPD	CCGCTCTTCTTGTGCAGTG	GGTAACCAGGCGTCCGATAC
AFP	TCTGAAACGCCATCGAAATGCC	AATGTAAATGTCGGCCAGTCCCT
LIVIN	CCGCATCTTCTTGTGCAGTG	GGTAACCAGGCGTCCGATAC

Normal Comet assay

The single cell gel electrophoresis (SCGE)/normal comet assay was carried out to assess the apoptotic cells as described by [47, 48]. Briefly, pieces of liver tissue from each animal of each experimental group were minced in 0.5 ml cold mincing solution, mixed with 0.5% low melting agarose (Sigma) and spread on frosted pre-coated slide with 1% normal melting agarose. After air drying, they were deep in cold lysis buffer for 1h in darkness. Following that, slides were incubated for 20 minutes at 4°C in TAE buffer (1x) then electrophoresed for 30 minutes at 300 mA and 25 V. and electrophoresed for 30 min at 24 V, then

washed with tap water twice before staining with ethidium bromide. Apoptotic cells characterized by large fan-like tails and small heads and intact cells were scored in one 50 cells per animal using fluorescent microscope (Carl Zeiss Axioplan with epifluorescence filter 15 BP546/12, FT580, and LP590). The extent of DNA migration in each sample was assessed using Ltd.'s Komet 5 image analysis software (Liverpool, UK). A Closed-Circuit Digital (CCD) camera was used to capture the images of comets.

Histopathological examination of liver tissue

For pathological examination, 10% formal saline was used as a fixative solution for liver tissue samples for 24 hours. Following the usual steps of

dehydration and embedding in paraffin wax, 4 μm tissue sections were cut before being dewaxed, rehydrated, and finally stained with hematoxylin and eosin (H and E) then viewed under light microscope for histological examination.

Statistical analysis

The current data were analyzed using (SPSS) version 18.0. To compare gene expression and DNA damage among groups, the Student's t-test or analysis of variance (ANOVA) were used. A P-value of <0.05 was considered statistically significant.

2. Results

Characterization of Au-NPs

High-resolution transmission electron microscope (HR-TEM) was utilized for Au-NPs characterization which revealed that these particles have an average size of 50.0 ± 2.0 nm with a long shape as shown in Figure 1A. Figure 1B shows the number frequency of particle size data in linear scale. The peak shows that the average size of Au-NPs is 69.67 nm, the Zeta potential of Au-NPs was shown with particles carrying a charge of 21.5mV. Zeta potential value was strongly positive (Figure 1C).

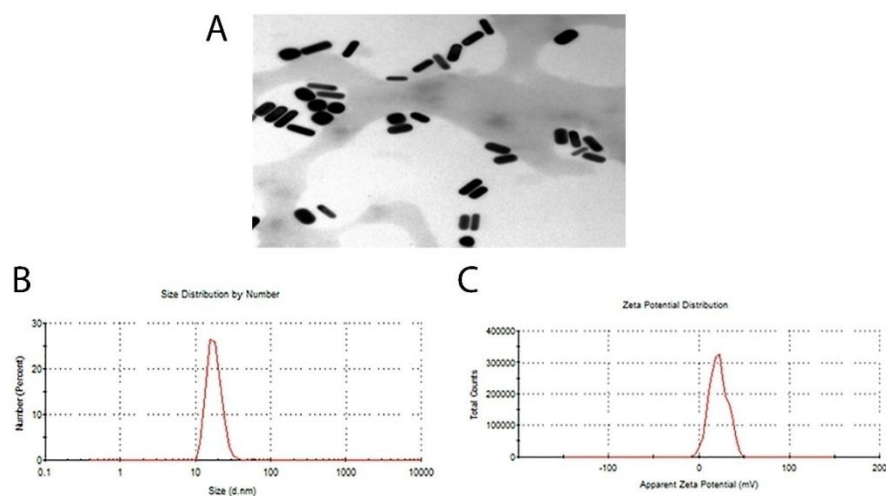


Figure 1: A: Image by HR-TEM image of the synthesized Au-NPs shows the rod shape of 50.0 ± 2.0 nm Au-NPs. B: Graph of particle size distribution of the synthesized AuNPs with average size 69.67 nm using particle size analyzer. C: Zeta potential of Au-NPs.

Quantitative analysis of mRNA expression

Treatment with Res and Au-NPs combination caused a significant ($p < 0.05$) downregulation of the

expression levels of AFP and Livin genes in Res-Au-NPs group in comparison with all other treated groups (Figure 2).

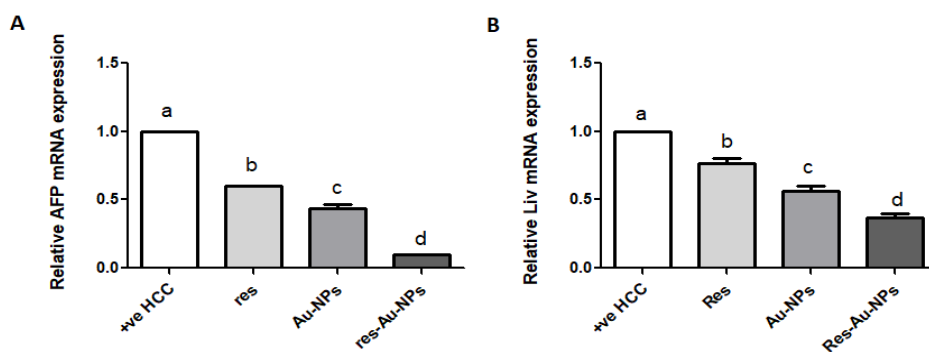


Figure 2: Quantitative analysis of mRNA expression of AFP (A) and Livin (B) genes using QRT-PCR extracted from liver tissue of HCC rat model treated with Res, Au-NPs and combination of Res and Au-NPs (Res-AuNPs). Expression levels were normalized to *GAPDH*. Data are expressed as the mean \pm SEM. * $P \leq 0.05$ compared with the control.

Normal Comet assay

Table 2,3 showed the effect of resveratrol and/or Au-NPs on DNA damage in liver tissues after one month and two months of induction. Group treated with Res- AuNPs resulted in statistically marked ($P \leq 0.05$) elevation parameters tail length, %DNA in tail and tail moment measurements in comparison to

those treated with Res alone or with Au-NPs. Moreover, it's obvious that prolonged treatment for two months caused further significant increase in the same parameters, where Res-AuNPs revealed the highest significant DNA damage in comparison to all other treated groups (Figure 3).

Table 2: Effect of resveratrol and/or Au-NPs on DNA damage in liver tissues after one month of induction

Groups	Tail length (μm) (Mean \pm SE)	% DNA in Tail (Mean \pm SE)	Tail Moment (μm) (Mean \pm SE)
-ve Res	3.48 \pm 0.13 ^{a, #}	2.21 \pm 0.24 ^{a, #}	0.071 \pm 0.02 ^{a, #}
-veHCC	3.57 \pm 0.12 ^{a, #}	2.3 \pm 0.26 ^{a, #}	0.081 \pm 0.01 ^{a, #}
HCC	7.04 \pm 0.08 ^{b, *}	4.5 \pm 0.14 ^{b, *}	0.3 \pm 0.01 ^{b, *}
Resv.	10.18 \pm 0.06 ^{c, *, #}	5.2 \pm 0.09 ^{b, *}	0.53 \pm 0.01 ^{c, *, #}
Au-NPs	10.20 \pm 0.17 ^{c, *, #}	5.19 \pm 0.85 ^{b, *}	0.53 \pm 0.08 ^{c, *, #}
Resv.+Au-NPs	14.6 \pm 0.05 ^{d, *, #}	7.24 \pm 0.06 ^{c, *, #}	1.05 \pm 0.01 ^{d, *, #}

-All values are represented as Mean \pm Standard error of mean (SE)

- There is a significant difference between groups by using one-way ANOVA at $P \leq 0.05$ followed by Duncan multiple comparison test.

- The same letter means that there is no significant difference between the two groups by using Duncan multiple comparison test ($P > 0.05$).

-The different letters mean that there is a significant difference between the two groups by using Duncan multiple comparison test ($P \leq 0.05$).

- * Statistically significant compared with normal (negative control) using student t- test.

- # Statistically significant compared with HCC (positive control) using student t- test.

Table 3: Effect of resveratrol and/or Au-NPs on DNA damage in liver tissues after two months of induction.

Groups	Tail length (μm) (Mean \pm SE)	% DNA in Tail (Mean \pm SE)	Tail Moment (μm) (Mean \pm SE)
-ve Res	3.12 \pm 0.08 ^{a, #}	3.54 \pm 0.19 ^a	0.13 \pm 0.01 ^a
-veHCC	3.23 \pm 0.09 ^{a, #}	3.67 \pm 0.15 ^a	0.15 \pm 0.02 ^a
HCC	4.96 \pm 0.49 ^{b, *}	4.82 \pm 0.43 ^a	0.46 \pm 0.15 ^{a, b}
Resv.	8.31 \pm 0.16 ^{c, *, #}	11.61 \pm 0.45 ^{b, *, #}	2.05 \pm 0.17 ^{c, *, #}
Au-NPs	11.49 \pm 0.72 ^{d, *, #}	4.13 \pm 0.67 ^a	0.52 \pm 0.06 ^{b, *}
Resv.+Au-NPs	18.23 \pm 0.45 ^{e, *, #}	7.34 \pm 1.15 ^{c, *, #}	1.59 \pm 0.07 ^{d, *, #}

-All values are represented as Mean \pm Standard error of mean (SE).

- There is a significant difference between groups by using one-way ANOVA at $P \leq 0.05$ followed by Duncan multiple comparison test.

- The same letter means that there is no significant difference between the two groups by using Duncan multiple comparison test ($P > 0.05$).

-The different letters mean that there is a significant difference between the two groups by using Duncan multiple comparison test ($P \leq 0.05$).

- * Statistically significant compared with normal (negative control) using student t- test.

- #Statistically significant compared with HCC (positive control) using student t- test.

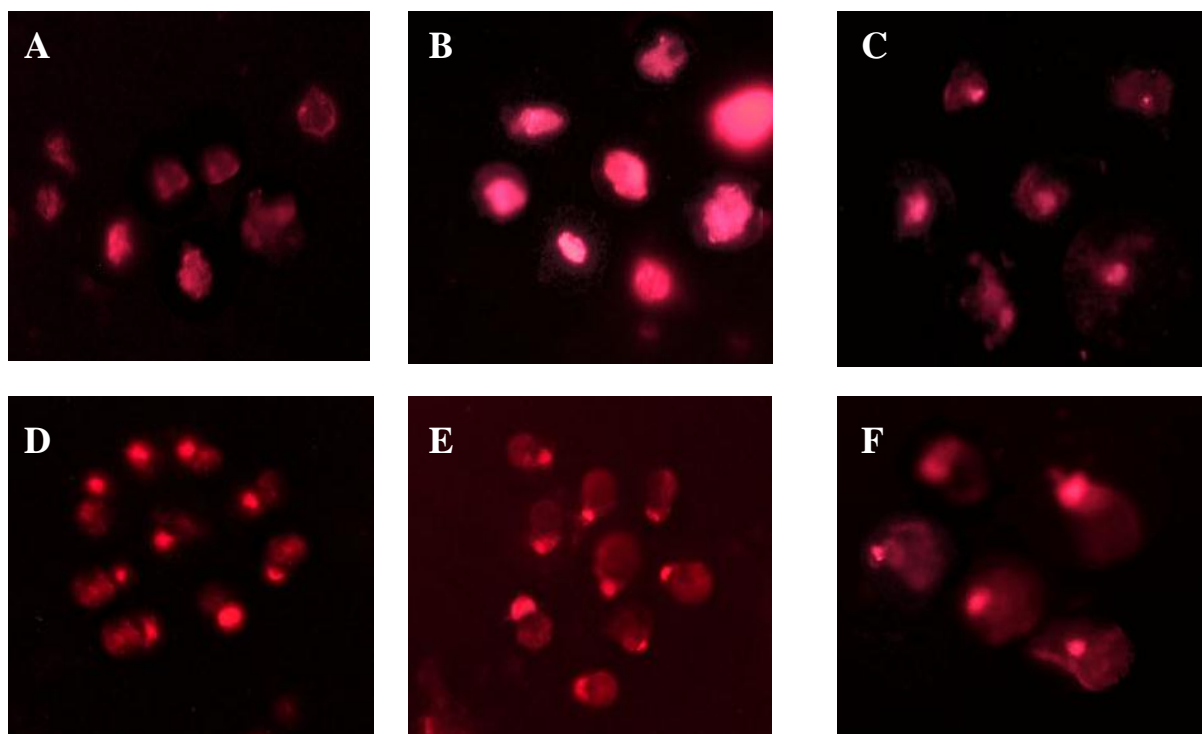


Figure 3: Representative photomicrographs showing typical nuclei with various degrees of DNA damage observed as comet induced by treating HCC with resveratrol or Au-NPs. Combined treatment induced the highest degree of DNA damage compared with undamaged DNA of control groups. A: -ve Res, B: -ve HCC, C: HCC, D: Res, E: Au-NPs and F: Res-Au-NPs. Magnification 400X.

Histopathological examination of the liver tissues

Histopathological examination of liver revealed normal parenchyma with normal portal area, hepatic artery, portal vein, central vein and blood sinusoid in both -ve Res and -ve HCC groups (Figure 4 A and B). While untreated HCC group showing diffuse hepatic degeneration, vacuolated hepatocytes, disorganized hepatic cords, congested central vein with hemorrhage and degenerated endothelial lining, pleomorphic nuclei and diffuse area of coagulative necrosis (Figure 4 C). Treatment with Res or Au-NPs decreased the degenerated hepatocytes with congestion in hepatoportal blood vessels with degenerated endothelial lining and degeneration in the adjacent hepatocytes (Figure 4 D and E). However, combined treatment with Res and Au-NPs demonstrated an improved hepatic parenchyma with

apparently normal hepatocytes and decrease in degenerated hepatocytes compared to HCC group (Figure 4F).

4. Discussion

As far as we know, there is no report on the efficiency of combined treatment with resveratrol and gold nanoparticles *in vivo*. Thus, in the present study we investigated the efficiency of simultaneous treatment with Res and Au-NPs as antitumor agents together against HCC and shed light on their possible synergistic effect on silencing livin gene.

Livin was reported to be highly expressed during early stages of HCC [49]. Interestingly, livin is not expressed in normal tissue while it is highly expressed in tumor cells, which rationalize the reason behind apoptotic induction in tumor cells only in response to down regulation of livin expression [50, 51].

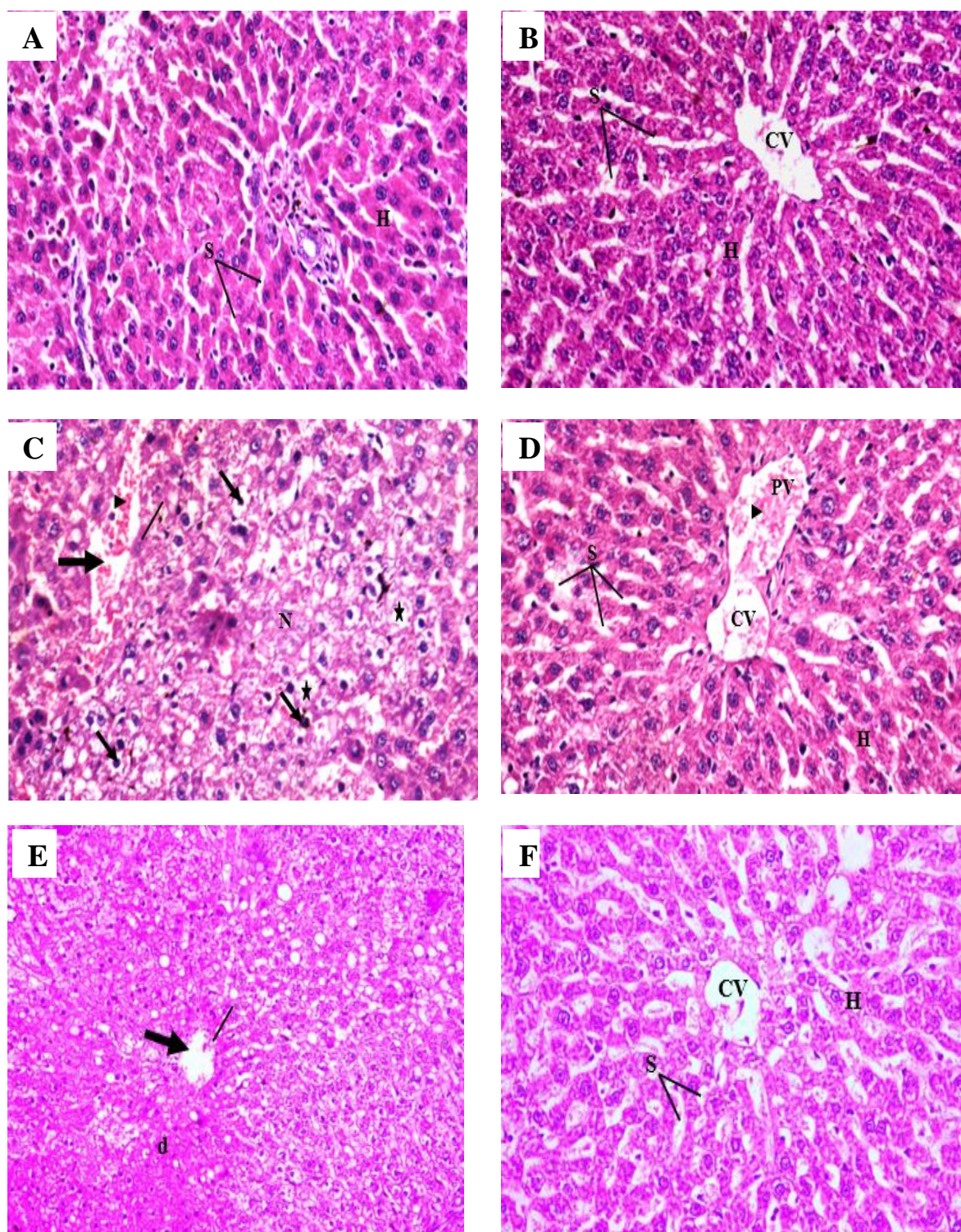


Figure 4: Photomicrographs for histopathological examination of liver sections of control and treated HCC rat model. A and B: (-ve Res and -ve HCC) showing normal hepatic architecture with normal portal area, hepatic artery, portal vein, blood sinusoid and bile duct (H and E X 400). C: (+ve HCC) showing diffuse hepatic degeneration, vacuolated hepatocytes (star) with disorganized hepatic cords, congested central vein (thick arrow) with haemorrhage (arrowhead) and degenerated endothelial lining (line), pleomorphic nuclei (arrows) and diffuse area of coagulative necrosis (N) (H and E X 400). D: Res treated group showing apparently normal hepatocytes, wide blood sinusoids, and haemorrhage in the portal vein (arrowhead) (H and E X 400). E: Au-NPs group showing decrease in the degenerated hepatocytes with severe congestion in hepatoportal blood vessel (thick

arrow) with degenerated endothelial lining (line) and degeneration in the adjacent hepatocytes (d) (H and E X 200). F: Res-Au-NPs group showing improved hepatic parenchyma with apparently normal hepatocytes, central vein and blood sinusoids (H and E X 400). H = hepatocytes, CV = central vein, S = sinusoids, N= necrosis.

This is in harmony with our findings, where livin expression reported a significant elevation in HCC group. Caspase is the target protein for Livin, where livin directly combines with it enabling other inhibitory apoptosis proteins (IAP) family members to combine with caspase via Smac/DIABLO protein which inhibit apoptosis of the cells [52, 53]. As the elevation of livin resulted in apoptosis inhibition, comet assay could confirm this suggestion by the low DNA damage percentage reported during first and second month in HCC group treated with diethyl nitrosamine to induce HCC model.

Our data revealed that an administration of Res could decrease livin expression and elevated the DNA damage in HCC induced rats (Res group), while normal cells in control groups (-ve HCC and -ve Res) showed intact DNA. Our findings agree with those of several authors who found that Resveratrol-loaded gold nanoparticles enhanced the anti-tumor effectiveness of free Res due to activating the intrinsic pathway of apoptosis and consequently could be a potential anti-tumor agent against pancreatic cancer cells [54]. Furthermore, a combination of resveratrol with matrine could induce significant antiproliferative properties by several mechanistic pathways one of them is through encouraging apoptosis via caspase-3 and caspase-9 activation [55]. Moreover, mitochondrial apoptosis has been reported as another mechanistic way of Res action [56]. These studies could rationalize the reported DNA damage in HCC due to elevation of livin, and intact DNA in normal cell because of silencing of livin gene and inhibition of oxidative DNA damage by Res [57].

Au-NPs could induce intracellular ROS mediated apoptosis that prevented the proliferation of HepG2 cells [58]. This also agrees with the recent findings stated that Au-NPs exerts its apoptotic effect through activation of Bax, Bid, caspases and inhibition of anti-apoptotic bcl-2 [59]. Our results are consistent with previous observations that have demonstrated that HCC induced rats treated with Au-NPs showed elevated apoptosis confirmed by increased tail length in Au-NPs treated group. However, the present study suggested another pathway for activation of apoptosis through inhibition of livin expression.

Taken together, simultaneous treatment with Res and Au-NPs could efficiently inhibit livin gene in Res-AuNPs group more than using each treatment separately, may be due to the synergetic effect of both which in turn could restore the apoptotic ability of the tumor cell. Many reports suggested that livin silencing reduced the apoptotic resistance in HCC cells with and diminishes markedly the propagation and invasiveness of HCC cells [60-62].

The efficiency of Res-AuNPs treatment could be assessed via measuring the expression level of AFP as being the most common diagnostic and prognostic tool for treated HCC [22]. The present findings revealed that Res-AuNPs group reported the most reduction of the AFP expression level in comparison to untreated HCC group.

Abnormal histological signs combined with HCC could significantly be improved after treatment either with Res or Au-NPs, whereas a combination of both has reported the most effective attenuation of the histological damaged of HCC. This may be attributed to the antioxidative effect of Res that prevent the oxidative DNA damage and enhance the antioxidant enzymes GSH and SOD and the anti-inflammatory effect represented by the decreased level of TNF α in liver tissue [57, 63]. For Au-NPs, recent studies have demonstrated their toxic effects in several organs via oxidative stress and interacting with cellular macromolecules inducing histocytotoxicity [64, 65], these effects were not obviously reported in our experiment may be because the effect of Au-NPs is dose, shape, and size dependent [65, 66].

5. Conclusion

our study has shown that the combination of resveratrol and gold nanoparticles was more efficient as an apoptotic inducer agent through inhibition of livin gene expression in hepatocellular carcinoma rat model which might be a prospective directed approach for the treatment of HCC.

5. Conflicts of interest

There are no conflicts to declare.

6. Formatting of funding sources

Funded by the Academy of Scientific Research and Technology (ASRT) scientists for next generation Programme (SNG)

7. Acknowledgments

This work was facilitated by the Genetics Laboratory, Zoology Department, Faculty of Science, Cairo University.

8. References

- Bray, F., et al., Global cancer statistics 2018: GLOBOCAN estimates of incidence and mortality worldwide for 36 cancers in 185 countries. 2018. **68**(6): p. 394-424.
- Rashed, W.M., et al., Hepatocellular Carcinoma (HCC) in Egypt: A comprehensive overview. 2020. **32**(1): p. 1-11.
- Gomaa, A.I., M.S. Hashim, and I. Waked, Comparing staging systems for predicting prognosis and survival in patients with hepatocellular carcinoma in Egypt. *PloS one*, 2014. **9**(3): p. e90929.
- Ibrahim, A.S., et al., Cancer incidence in Egypt: results of the national population-based cancer registry program. 2014. **2014**.
- Abd-Elsalam, S., et al., Epidemiology of liver cancer in Nile delta over a decade: a single-center study. 2018. **7**(01): p. 24-26.
- Liu, H., et al., Inhibition of tumorigenesis and invasion of hepatocellular carcinoma by siRNA-mediated silencing of the livin gene. *Mol Med Rep*, 2010. **3**(6): p. 903-7.
- Dasgupta, A., et al., Expression and functional role of inhibitor-of-apoptosis protein livin (BIRC7) in neuroblastoma. 2010. **400**(1): p. 53-59.
- Xi, R.C., et al., Significant elevation of survivin and livin expression in human colorectal cancer: inverse correlation between expression and overall survival. 2011. **34**(8-9): p. 428-432.
- Byers, N.M., R.L. Vandergaast, and P.D.J.J.o.V. Friesen, Baculovirus inhibitor-of-apoptosis Op-IAP3 blocks apoptosis by interaction with and stabilization of a host insect cellular IAP. 2016. **90**(1): p. 533-544.
- Augello C, C.L., Maggioni M, et al: Inhibitors of apoptosis, p.I.e.a.t.p.s. in, and hepatocellular carcinoma. *BMC Cancer* 9: 125, Inhibitors of apoptosis proteins (IAPs) expression and their prognostic significance in hepatocellular carcinoma. *BMC Cancer* 2009. **125**(9).
- Myung, D.-S., et al., Expression of Livin in colorectal cancer and its relationship to tumor cell behavior and prognosis. 2013. **8**(9): p. e73262.
- Durinck, S., et al., Spectrum of diverse genomic alterations define non-clear cell renal carcinoma subtypes. 2015. **47**(1): p. 13-21.
- Liu, K., et al., BIRC7 promotes epithelial-mesenchymal transition and metastasis in papillary thyroid carcinoma through restraining autophagy. 2020. **10**(1): p. 78.
- Altieri, B., et al., Livin/BIRC7 expression as malignancy marker in adrenocortical tumors. 2017. **8**(6): p. 9323.
- Yang, Y., et al., High BIRC7 expression might be an independent prognostic indicator of poor recurrence-free survival in patients with prostate cancer. 2018. **17**: p. 1533033818809694.
- Cho, S.B., et al., Livin is associated with the invasive and oncogenic phenotypes of human hepatocellular carcinoma cells. 2015. **45**(4): p. 448-457.
- Badr, E.A., et al., A correlation between BCL-2 modifying factor, p53 and livin gene expressions in cancer colon patients. 2020. **22**: p. 100747.
- Zhang, Z., et al., The clinicopathological and prognostic significances of IGF-1R and Livin expression in patients with colorectal cancer. 2022. **22**(1): p. 1-11.
- Badr, E.A., et al., A pilot study of Livin gene and Yes-associated protein 1 expression in hepatocellular carcinoma patients. 2019. **5**(11): p. e02798.
- Moldogazieva, N.T., et al., Predictive biomarkers for systemic therapy of hepatocellular carcinoma. 2021. **21**(11): p. 1147-1164.
- Yang, S., et al., Preoperative serum α -fetoprotein and prognosis after hepatectomy for hepatocellular carcinoma. 2016. **103**(6): p. 716-724.
- Jasirwan, C.O.M., et al., The alpha-fetoprotein serum is still reliable as a biomarker for the surveillance of hepatocellular carcinoma in Indonesia. *BMC Gastroenterology*, 2020. **20**(1): p. 215.
- Gupta, D.S., et al., Resveratrol and Its Role in the Management of B-Cell Malignancies—A Recent Update. 2023. **11**(1): p. 221.
- Angellotti, G., et al., Chemopreventive and Anticancer Role of Resveratrol against Oral Squamous Cell Carcinoma. 2023. **15**(1): p. 275.
- Gupta, N., et al., Safety and efficacy of combined resveratrol and sirolimus in lymphangioleiomyomatosis. 2023.
- Liu, X., et al., Gold Nanoparticles Functionalized with Au–Se-Bonded Peptides Used as Gatekeepers for the Off-Target Release of Resveratrol in the Treatment of Triple-Negative Breast Cancer. 2023.
- Ferraresi, A., et al., Resveratrol inhibits IL-6-induced ovarian cancer cell migration through epigenetic up-regulation of autophagy. 2017. **56**(3): p. 1164-1181.

28. Esposito, A., et al., Resveratrol Contrasts IL-6 Pro-Growth Effects and Promotes Autophagy-Mediated Cancer Cell Dormancy in 3D Ovarian Cancer: Role of miR-1305 and of Its Target ARHI. 2022. **14**(9): p. 2142.
29. Ferraresi, A., et al., The protein restriction mimetic Resveratrol is an autophagy inducer stronger than amino acid starvation in ovarian cancer cells. 2017. **56**(12): p. 2681-2691.
30. Thongchot, S., et al., Resveratrol interrupts the pro-invasive communication between cancer associated fibroblasts and cholangiocarcinoma cells. 2018. **430**: p. 160-171.
31. Vallino, L., et al., Modulation of non-coding RNAs by resveratrol in ovarian cancer cells: In silico analysis and literature review of the anti-cancer pathways involved. 2020. **10**(3): p. 217-229.
32. Vidoni, C., et al., Glycolysis Inhibition of Autophagy Drives Malignancy in Ovarian Cancer: Exacerbation by IL-6 and Attenuation by Resveratrol. 2023. **24**(2): p. 1723.
33. Li, B., et al., Resveratrol sequentially induces replication and oxidative stresses to drive p53-CXCR2 mediated cellular senescence in cancer cells. 2017. **7**(1): p. 1-12.
34. Afrin, S., et al., Dietary phytochemicals in colorectal cancer prevention and treatment: A focus on the molecular mechanisms involved. 2020. **38**: p. 107322.
35. Cheng, Z., et al., Nanomaterials for cancer therapy: Current progress and perspectives. 2021. **14**(1): p. 1-27.
36. Cao, L., et al., Emerging nano-based strategies against drug resistance in tumor chemotherapy. 2021: p. 1255.
37. Golombek, S.K., et al., Tumor targeting via EPR: Strategies to enhance patient responses. 2018. **130**: p. 17-38.
38. Minassian, G., et al., Gold Nanoparticles Conjugated with Dendrigraft Poly-L-lysine and Folate-Targeted Poly (ethylene glycol) for siRNA Delivery to Prostate cancer.
39. Baran, A.J.P.S. and Technology, Inhibitory effects of gold nanoparticles biosynthesized by redox reaction using Rheum ribes lam fruit peels on pathogen strains and cancer cells. 2023: p. 1-12.
40. Dickson, J., et al., Anti-neoplastic Effects of Gold Nanoparticles Synthesized Using Green Sources on Cervical and Melanoma Cancer Cell Lines. 2023: p. 1-9.
41. Shochah, Q.R., F.A.J.B.C. Jabir, and Biorefinery, Green synthesis of Au/ZnO nanoparticles for anticancer activity and oxidative stress against MCF-7 cell lines. 2023: p. 1-14.
42. Shen, J., et al., Multifunctional gold nanorods for siRNA gene silencing and photothermal therapy. 2014. **3**(10): p. 1629-1637.
43. Bonoiu, A.C., et al., Gold nanorod-siRNA induces efficient in vivo gene silencing in the rat hippocampus. 2011. **6**(4): p. 617-630.
44. Conde, J., et al., Gold-nanobeacons for simultaneous gene specific silencing and intracellular tracking of the silencing events. 2013. **34**(10): p. 2516-2523.
45. Turkevich, J., P.C. Stevenson, and J. Hillier, A study of the nucleation and growth processes in the synthesis of colloidal gold. Discussions of the Faraday Society, 1951. **11**: p. 55-75.
46. Yuan, J.S., et al., Statistical analysis of real-time PCR data. BMC bioinformatics, 2006. **7**(1): p. 1-12.
47. Kizilian, N., et al., Silver-stained comet assay for detection of apoptosis. 1999. **27**(5): p. 926-930.
48. Attia, S.M., et al., Proanthocyanidins produce significant attenuation of doxorubicin-induced mutagenicity via suppression of oxidative stress. 2010. **3**(6): p. 404-413.
49. Wyllie, A.H.J.C. and C. Physiology, Cell death. 1987: p. 755-785.
50. Lazar, I., et al., The clinical effect of the inhibitor of apoptosis protein livin in melanoma. 2012. **82**(4): p. 197-204.
51. Guo, H., et al., Expression and clinical significance of livin protein in hepatocellular carcinoma. 2013. **35**(5): p. 489-496.
52. Vucic, D., et al., Engineering ML-IAP to produce an extraordinarily potent caspase 9 inhibitor: implications for Smac-dependent anti-apoptotic activity of ML-IAP. 2005. **385**(1): p. 11-20.
53. Ma, L., et al., Livin promotes Smac/DIABLO degradation by ubiquitin-proteasome pathway. 2006. **13**(12): p. 2079-2088.
54. Lee, D.G., et al., Resveratrol-loaded gold nanoparticles enhance caspase-mediated apoptosis in PANC-1 pancreatic cells via mitochondrial intrinsic apoptotic pathway. Cancer Nanotechnology, 2022. **13**(1): p. 1-19.
55. Ou, X., et al., Potentiation of resveratrol-induced apoptosis by matrine in human hepatoma HepG2 cells. 2014. **32**(6): p. 2803-2809.
56. Dai, Z., et al., Antitumor effect of resveratrol on chondrosarcoma cells via phosphoinositide 3-kinase/AKT and p38 mitogen-activated protein kinase pathways Retraction in/10.3892/mmr. 2021.12238. 2015. **12**(2): p. 3151-3155.
57. Türkmen, N.B., et al., Protective effect of resveratrol against pembrolizumab-induced hepatotoxicity and neurotoxicity in male rats. 2022: p. e23263.

58. Nandhini, J.T., D. Ezhilarasan, and S.J.E.t. Rajeshkumar, An ecofriendly synthesized gold nanoparticles induces cytotoxicity via apoptosis in HepG2 cells. 2021. **36**(1): p. 24-32.
59. Ji, Y., et al., Green synthesis of gold nanoparticles using a *Cordyceps militaris* extract and their antiproliferative effect in liver cancer cells (HepG2). 2019. **47**(1): p. 2737-2745.
60. Liu, H., et al., Inhibition of tumorigenesis and invasion of hepatocellular carcinoma by siRNA-mediated silencing of the livin gene. 2010. **3**(6): p. 903-907.
61. Li, G., et al., Targeted silencing of inhibitors of apoptosis proteins with siRNAs: a potential anti-cancer strategy for hepatocellular carcinoma. 2013. **14**(9): p. 4943-4952.
62. Pu, Z., et al., Matrine induces cell cycle arrest and apoptosis in hepatocellular carcinoma cells via miR-122 mediated CG1/livin/survivin signal axis. 2021. **20**(2): p. 263-268.
63. Abdelrahman, S.A., et al., Histomorphological changes and molecular mechanisms underlying the ameliorative effect of resveratrol on the liver of silver nanoparticles-exposed rats. 2022: p. 1-17.
64. Jarrar, Q., et al., On the toxicity of gold nanoparticles: Histological, histochemical and ultrastructural alterations. 2022. **38**(12): p. 789-800.
65. Fadia, B.S., et al., Histological Injury to Rat Brain, Liver, and Kidneys by Gold Nanoparticles is Dose-Dependent. 2022.
66. Wang, S., et al., Challenge in understanding size and shape dependent toxicity of gold nanomaterials in human skin keratinocytes. 2008. **463**(1-3): p. 145-149.